Wageningen University – Department of Genetics

MSc Thesis Chair Group Genetics

Expanding the Resistance Spectrum: Non-Azole Challenges in *Aspergillus fumigatus*

Date: March 13, 2024
Thesis code: GEN-80436
Student: Andrea Cristina Molina Almeida
Program: Master Biotechnology
Specialization: Cellular and Molecular Biotechnology
Supervisors: Ben Auxier
Examiners: Ben Auxier and Eveline Snelders

Table of Contents

1 Abstract

In agricultural settings, *Aspergillus fumigatus* is exposed to a wide range of antifungals commonly employed for plant pathogen management. This exposure has led to the emergence of fungal strains that are no longer susceptible to certain chemicals, notably azoles, which are of clinical significance. Despite recognizing resistance in a few multidrug-resistant samples, research into resistance against fungicides lacking clinical relevance, yet commonly used in agriculture, remains insufficient. It is crucial to enhance our understanding of the mechanisms behind this newly observed resistance, as it may threaten the success of future treatments for aspergillosis.

Through genetic analysis and evaluations of fungicide susceptibility, employing techniques such as sexual crossing, next-generation sequencing, and bulk segregant analysis, give a preliminary insight into this newly described mechanism hidden inside the genome of the fungi. This research led to the discovery of two significant quantitative trait loci on chromosomes 1 and 6, revealing a complex genetic interaction contributing to this loss of susceptibility to non-azole fungicides. These loci were also linked to traits influencing growth size and sporulation, suggesting a close genetic interaction between these phenotypic attributes and the newly described resistance mechanisms in *A. fumigatus* under environmental pressure.

These findings underline the necessity to increase the studies of fungal resistance to non-clinically relevant fungicides. Identifying candidate genes within these regions opens opportunities for future research, including employing various sequencing technologies and examining candidate gene function through CRISPR-Cas9 editing.

2 List of Abbreviations

BN	Big non-sporulate
BS	Big sporulate
BSA	Bulk segregant analysis
CM	Complete medium
CTAB	Cetrimonium bromide
EDTA	Ethylenediaminetetraacetic acid
gDNA	Genomic DNA
QoI	Quinone outside inhibitors
QTL	Quantitative trait locus
MBC	Methyl benzimidazole carbamate
MQ	Milli-Q water
MM	Minimal medium
OD	Optical density
SdhI	Succinate dehydrogenase inhibitors
SN	Small non-sporulate
SS	Small sporulate

3 Introduction

Aspergillus fumigatus, a saprophytic fungus prevalent in decaying plant material (Schoustra et al., 2019), engages in both asexual and sexual reproduction (Zhang et al., 2021). Its predominant method of propagation, asexual reproduction involves the generation of conidia within specialized structures called conidiophores, which are dispersed into the air upon reaching maturation (Van De Veerdonk et al., 2017). *A. fumigatus* is also capable of sexual reproduction, characterized by the formation of cleistothecia. However, this process is infrequently observed in natural environments because it requires specific conditions, such as prolonged darkness, specialized nutrients, and elevated temperatures, to occur (O'Gorman et al., 2009). Thus, the mode of sexual reproduction is believed to only take place under unfavorable conditions to confer an evolutionary advantage to fungi by conferring a wider genetic diversity (Van De Veerdonk et al., 2017, Zhang et al., 2021).

As an opportunistic pathogen, *A. fumigatus* represents a significant threat to immunocompromised and immunosuppressed individuals due to its reproductive and dispersal mechanism, allowing it to be present in almost all settings (Schoustra et al., 2019). The ubiquitous presence of airborne conidia in the environment makes susceptible individuals vulnerable to various forms of aspergillosis. It is estimated that each year, these infections contribute to approximately 3,000,000 cases of chronic pulmonary aspergillosis and 250,000 cases of invasive aspergillosis worldwide (Bongomin et al., 2017).

The treatment of aspergillosis predominantly depends on the efficacy of triazole antifungals, making the emergence of azole-resistant *A. fumigatus* strains of significant relevance (Khateb et al., 2023). The continuous increase in azole-resistant fungi, particularly noted in the Netherlands, where instances of resistance have doubled in the last decade, emphasizes the growing concerns regarding future aspergillosis treatment strategies (Lestrade et al., 2020). Initial clinical cases of azole resistance in *A. fumigatus* were linked to prolonged azole therapies (Hagiwara et al., 2016). However, the continuous and rapid rise in resistant cases among patients not previously exposed to azole treatments suggests the existence of a secondary source for developing resistance outside of clinical settings (Berger et al., 2017), pinpointing agricultural practices as a contributory factor. Specifically, compost piles, where *A. fumigatus* comes into close contact with other phytopathogenic fungi, and the fungicides aimed at controlling them (Greeff & Mouton, 2017), creating a focal point for the emergence of azole-resistant strains.

Resistance to azoles in *A. fumigatus* is primarily due to mutations in the cytochrome P450 14α-demethylase enzyme, which is essential for ergosterol synthesis and thus critical for maintaining fungal cell membrane structure (Zhang et al., 2019). The most common mutations associated with azole resistance occur in the cyp51A gene, leading to amino acid substitutions or gene overexpression, either through point mutations or tandem repeats (MacEdo et al., 2020). These genetic modifications disrupt ergosterol production (Assress et al., 2021). However, azole

resistance mechanisms extend beyond the *cyp51A* gene, encompassing genes such as *hmg1* and *erg6,* as well as some transcriptional factors, such as *hapE*, or the overexpression of drug efflux pumps (Gonzalez-Jimenez et al., 2020). Despite being attributed to having two different origins for their azole resistance, clinical and environmental isolates exhibit significant genetic relatedness, contrary to what has been observed between azole-resistant and azole-sensitive populations (Rhodes et al., 2022; Snelders et al., unpublished.).

Nevertheless, fungicides used in agricultural settings extend beyond azoles to include other antifungal classes, such as Methyl Benzimidazole Carbamate (MBC) antifungals, Quinone Outside Inhibitors (QoI), Succinate Dehydrogenase Inhibitors (SDHI), and Morpholines (Brauer et al., 2019; Snelders et al., unpublished.). As such, this implies that on compost piles *A. fumigatus* may have not only developed resistance to azoles but could also exhibit reduced sensitivity towards other fungicides. Despite the critical nature of this issue, research into resistance against a broader spectrum of antifungals used in agriculture remains limited. The few studies that dig into this topic already warn about the identification of some samples of *A. fumigatus*, from an agricultural origin, displaying resistance across multiple fungicide classes, including MBC, QoI, and SdhI (Fraaije et al., 2020; Gonzalez-Jimenez et al., 2021; Kang et al., 2022). However, even with extensive research on azole resistance in *A. fumigatus*, our understanding of the resistance mechanisms to non-azole antifungals is still lacking. Such ignorance on the topic could be detrimental if *A. fumigatus* already has acquired resistance mechanisms to a wider array of fungicides, some of whom might be considered for future aspergillosis treatment strategies.

Preliminary investigations, through quantitative trait locus (QTL) analysis on offspring from sexual crosses between azole-resistant and azole-sensitive *A. fumigatus* isolates, have provided speculative evidence suggesting that resistance to non-azole fungicides might be linked to specific mutations on chromosome 5, a region not previously known to be implicated in any form of antifungal resistance (Snelders et al., unpublished). Furthermore, the discovery of this region's association with newly identified resistance reported a potential fitness trade-off in strains harboring these mutations, especially evident in environments devoid of antifungal agents (Bastos et al., 2021; Snelders et al., unpublished). This phenomenon, known as a fitness cost, occurs when mutations conferring fungicide resistance also disrupt other physiological and biochemical processes, leading to survival disadvantages in the absence of the fungicide compared to wild-type strains (Anderson, 2005). Potential areas impacted by this fitness cost include but are not limited to, spore production and dispersal, infection efficiency, mycelial growth, and competition with non-resistant wild strains (Mikaberidze & McDonald, 2015).

The research by Snelders et al. (unpublished) shows one of the first explorations into understanding the genetic foundations of antifungal resistance beyond azoles in *A. fumigatus.* By identifying a potential QTL within a specific chromosomal region, this work proposes that resistance to a broader spectrum of antifungals might be genetically encoded outside of the known resistance mechanisms related to azoles. As well, this discovery paves the way for further research into

compensatory mechanisms that may mitigate the fitness costs commonly linked to resistance, helping to understand the evolutionary dynamics of the fungi. The challenge moving forward focuses on validating the identified QTLs' contributions to antifungal resistance and determining their effects on the fitness of the organism. It also implies a screening against non-clinically relevant antifungals, for which the establishment of methodologies to evaluate susceptibility to a range of antifungals is not covered by the current clinical guidelines, highlighting a gap in the existing protocols of the European Committee on Antimicrobial Susceptibility Testing (Fraaije et al., 2020; Gonzalez-Jimenez et al., 2021; Guinea et al., 2019).

Given the critical implications of multi-fungicide resistance in *A. fumigatus*, this research is pivotal for future aspergillosis management strategies. It seeks to address the following question: What are the genetic mechanisms underlying resistance to non-azole antifungals in *Aspergillus fumigatus*, and are mutations on specific chromosomal regions associated with this resistance while considering potential fitness costs associated with it? It is expected that genes or genes in a specific chromosomal region cause resistance to non-azole antifungals in these fungi and it may also be correlated with a fitness cost in resistant strains. As such, various chemical agents will be tested against it, to examine potential correlations between resistance and phenotypic changes, aiming to advance the understanding of the genetic basis of non-azole antifungal resistance.

4 Material & Method

4.1 Source Strains.

The two parental strains 46A23 (azole-resistance) and 88C19 (azole-sensible) are among the175 *A. fumigatus* isolates part of an NWO Green III funded project entitled "*One health consequences of circularity; What lessons to learn from the saprophytic and human pathogenic fungus A. fumigatus*?" (Project number GROEN.2019.002) The project aimed to compile a balanced collection of isolates, with half being environmental and the other half clinical, all sourced from the Netherlands. Additionally, two laboratory-stored strains, AFIR974 and AFIR964, were chosen as experimental controls.

4.2 Sexual Cross

Before the beginning of the project, crosses between the azole-resistant strain 46A23 and the azole-sensitive strain 88C19 were performed. The cross was performed on oatmeal agar. The cross involved a heat shock step, followed by sealing the cultures in parafilm and incubating at 30°C in darkness for 2 months until cleistothecia formation was observed (Ashton & Dyer, 2019). To prepare the spore suspension (C001), the cleistothecia were collected from slants using cotton swabs and suspended in a solution of Milli-Q water (MQ) with 0.05% Tween (Tween-80). The suspension was then stored for at least one year before the initiation of the project.

4.3 Viability and Quantification of Spores

To confirm spore viability, 60 µL of the C001 spore suspension, along with the parental strains 88C19 and 46A23 and two control strains, AFIR974 and AFIR964, were cultured in duplicate in Complete Medium (CM) supplemented with 1% Triton, to prevent clumping, and incubated for 48 hours at 37°C. After confirming the viability of all strains, the CASY cell counter was then used to quantify the conidia in each sample. Subsequently, dilutions were prepared to achieve a final concentration of 5 × 10^5 conidia/mL in solutions of MQ water with 0.05% Tween-80.

4.4 Phenotype Groupings of C001

C001 spores were cultivated on eight plates containing CM supplemented with 1% Triton, with 50 µl of spore suspension added to each plate, and incubated for 48 hours at 37°C The growth areas of the isolates on these plates were quantified using ImageJ software (Additional Material 1) Isolates were classified based on two criteria: growth area and sporulation color, identifying four distinct phenotypes: big spores with green sporulation (BS), small spores with green sporulation (SS), big spores with no sporulation (BN), and small spores with no sporulation (SN).

For each phenotype, ten samples were selected and cultured on slant tubes containing Minimal Medium (MM) agar. Following a 96-hour incubation period at 37°C, all isolates were transferred using a cotton swab into a solution of MQ water with 0.05% Tween-80, with each sample adjusted to a concentration of $5x10^5$ conidia.

4.5 Fungicide Susceptibility Test Against Parental Strains

To assess the susceptibility of *A. fumigatus* strains to various antifungal agents, gradient agar plates containing CM and high concentrations of each chemical were prepared for both parental strains and the controls. The method involved pouring two linear layers at different angles of CM agar on opposite sides of each plate, one with and the other without the antifungal agent, to create a concentration gradient through diffusion.

A detailed list of the antifungal agents and their maximum concentrations is provided in Annex 1. The selection of antifungal chemicals was based on several criteria including their agricultural relevance in the Netherlands, availability within our laboratory, and the goal to include representatives from each major class of antifungal agents, as categorized by the Fungicide Resistance Action Committee (FRAC, 2023; Snelders et al., unpublished.).

Twelve antifungal agents were selected for this study: itraconazole, voriconazole, posaconazole, tebuconazole, azoxystrobin, benomyl, propamocarb, mancozeb, copper (II) sulfate pentahydrate, copper (II) sulfate anhydrous, acriflavine, and carvacrol. Concentrations for clinically relevant azoles were determined following established susceptibility detection methods (Guinea et al.,

2019). For other chemicals, lacking well-established tests, concentrations were based on recent *A. fumigatus* research and susceptibility findings in closely related species (Auxier et al., 2023; Kocić-Tanackov et al., 2012; Piprotar et al., 2022; Snelders et al., unpublished.; Song et al., 2019; Y. Zhang et al., 2023)

After 48 hours of incubation, observations focused on differences in growth and sporulation between azole-resistant and non-azole-resistant parental strains of *A. fumigatus.* Fungicides showing a differential effect on the azole-resistant parent, but not on the non-azole-resistant parent, or those causing noticeable phenotypic changes, such as alterations in color or sporulation, were selected for further testing against the offspring.

4.6 Fungicide Susceptibility Test Against Sexual Offspring

Following the differences in the parental strains, a subset of antifungals was chosen for further testing on the progeny groups: itraconazole, tebuconazole, benomyl, mancozeb, and acriflavine. For each antifungal, two concentrations were selected to discern susceptibility variations among the offspring exhibiting distinct phenotypes. The lower concentration was determined as the highest at which the azole-resistant parental strain could grow without visible phenotypic alterations, indicating persistence. Meanwhile, the higher concentration was chosen based on the point at which the azole-resistant parental strain either was not able to grow or exhibited significant phenotypic changes, such as alterations in the growth area, color, or sporulation absence.

Ten isolates representing each of the four phenotypes identified from the sexual cross (BS, SS, BN, SN), alongside the parental strains, underwent susceptibility testing. Each isolate inoculated with 50 µl onto CM agar containing the two different antifungal concentrations, was incubated at 37°C, with duplicates prepared for each test to ensure reproducibility. After 48 hours of incubation, the growth area of each isolate was quantified using ImageJ software, and any relevant characteristics, such as lack of sporulation and potential contamination, were annotated. Annex 2 contains the antifungal agents, their concentrations, the average growth areas, and spore production percentages.

Statistical analyses were conducted using RStudio (Version 2023.12.1+402), applying Wilcoxon and Kruskal-Wallis tests to assess differences in sporulation and growth across the tested antifungals and concentrations for each phenotype within C001 and parental, as well as in comparison to control samples not exposed to antifungals.

4.7 DNA Isolation

Mycelial mats for DNA extraction were produced by placing cellulose dialysis films (order no. 330-95) over CM agar to isolate each phenotype, resulting in four mycelial mats per phenotype, encompassing 16 isolates each. These mats were harvested after 24 hours and ground into a fine

powder using liquid nitrogen, a mortar, and a pestle, then stored in 15 mL safelock tubes at -80°C until DNA extraction.

For DNA extraction, 0.2 g of each sample was transferred into 1.5 ml Eppendorf tubes containing 500 µl CTAB buffer (CTAB, NaCl, 1M Tris, and 0.5 M EDTA). The mixture was vortexed to achieve a homogeneous solution and then incubated at 65°C for 1 hour. After cooling for 2-3 minutes at room temperature, 500 µL of chloroform: isoamyl alcohol (24:1) was added. The mixture was vortexed and centrifuged at 13,250 rpm for 15 minutes.

While the centrifugation was ongoing, 1.5 ml Eppendorf tubes containing 300 µl of ice-cold isopropanol were prepared. The aqueous phase from the centrifuged samples was transferred to pre-prepared tubes and stored at -20°C for at least 2 hours to precipitate DNA. Following another round of centrifugation under the same conditions, the supernatant was discarded. The DNA pellet was washed with 200 µL of 96% ethanol, vortexed, and centrifuged again at 13,250 rpm for 5 minutes to remove impurities. This wash step was repeated, and residual ethanol was evaporated by air-drying the tubes in a fume hood for 15-30 minutes.

The dried DNA pellet was resuspended in 50 µL of MQ water. To remove RNA, 50 µL of RNase was added and the sample was incubated overnight. RNA removal and final DNA purification were conducted using the SPRI beads protocol (see Additional Material 2).

4.8 Quality Control of Samples and Sequencing

The DNA concentration for each sample was quantified using the Qubit Fluorometer (Thermo Fisher Scientific), following the manufacturer's instructions. This involved preparing a Qubit working solution by diluting Qubit reagent with buffer at a ratio of 1:200. The solution was prepared for two standards and the four samples, which were then vortexed, briefly incubated, and measured under the dsDNA Broad Range setting on the Qubit Fluorometer. Subsequently, to evaluate the purity of the DNA samples, the absorbance ratios (A260/A280 and A260/A230) were measured using a NanoDrop Spectrophotometer (DeNovix Spectrophotometer).

Gel electrophoresis was performed, to verify the integrity of the extracted DNA. Samples were run on a 1% agarose gel containing ethidium bromide at 100V and 400 mA for one hour. A 10kb DNA ladder (Promega) was included to provide a molecular weight reference, facilitating the assessment of DNA quality.

Afterward, DNA sequencing was performed using the Oxford Nanopore Technologies platform. The sequencing protocol employed was the native barcoding of genomic DNA (gDNA) using the Native Barcoding Kit 24 V14 (SQK-NBD114.24) for Adaptive Sampling (Anderson et al., 2023). The MinION sequencing was conducted for a continuous period of 72 hours.

4.9 Bioinformatic Analysis of Sequencing Data

This study's sequencing analysis integrated barcoding sequencing data from Oxford Nanopore Technologies' MinION system and Illumina sequencing data previously acquired from Novogene for a distinct project. To align sequences, reference genomes such as Af293 (ASM265v1), A1160 (ASM2422042v1), Afir964 (ASM2875220v1), and Afir974 (ASM2875217v1) were selected and processed using the Terminal command line interface.

Given the different origins of the datasets, distinct alignment methodologies were applied. MinION sequence reads were aligned to the reference genomes using minimap2, with duplicates identified post-alignment through sorting and compression steps using GATK. Variant calling was performed using BCFtools and GATK for these reads. In contrast, Illumina sequence data were aligned using the BWA-MEM algorithm, with SAMtools facilitating duplicate identification after sorting and compression. Variant calling for the Illumina dataset also utilized GATK and BCFtools.

All variant data were then transferred into Rstudio, where the QTLseqr and ggplot2 packages were employed. These tools facilitated the identification of QTLs correlating to the variants of interest in the samples, alongside the computation of QTL-seq and G' statistical approaches by performing the bulk segregant analysis (BSA).

5 Results

5.1 Parental and Offspring Phenotypes

Before the start of this study, sexual crosses were performed between azole-resistant and azole-sensitive *A. fumigatus* isolates. It was essential first to confirm the viability of the resulting sexual cross (C001). The sample demonstrated viability within two days of incubation. This cross yielded a diverse array of offspring, categorized into four distinct phenotypes for this experiment, as depicted in Figure 1.

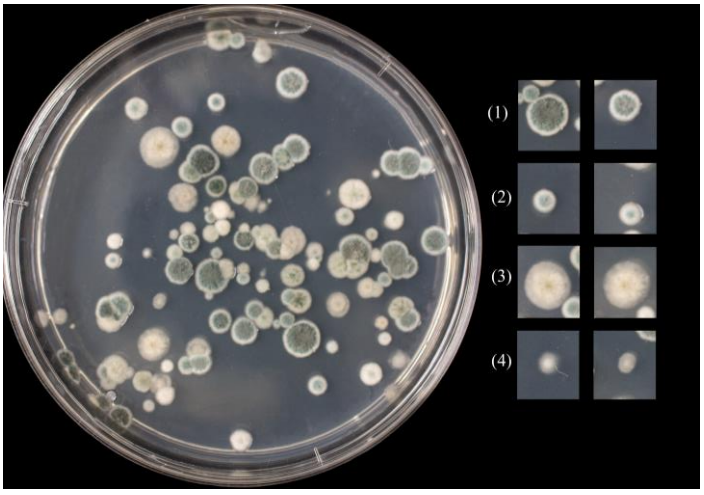

Figure 1: Phenotypic Diversity Among Offspring (C001) from Sexual Crosses of A. fumigatus on CM Agar. *This study identified four distinct phenotypes: (1) large isolates with sporulation (BS), characterized by a larger growth area and green sporulation compared to the other isolates; (2) small-sized offspring with sporulation (SS), showing a reduced colony size yet maintaining green sporulation; (3) large isolates without sporulation (BN), demonstrate typical growth but lacking green spores; and (4) small isolates without sporulation (SN), which are reduced in both size and devoid of green spores*.

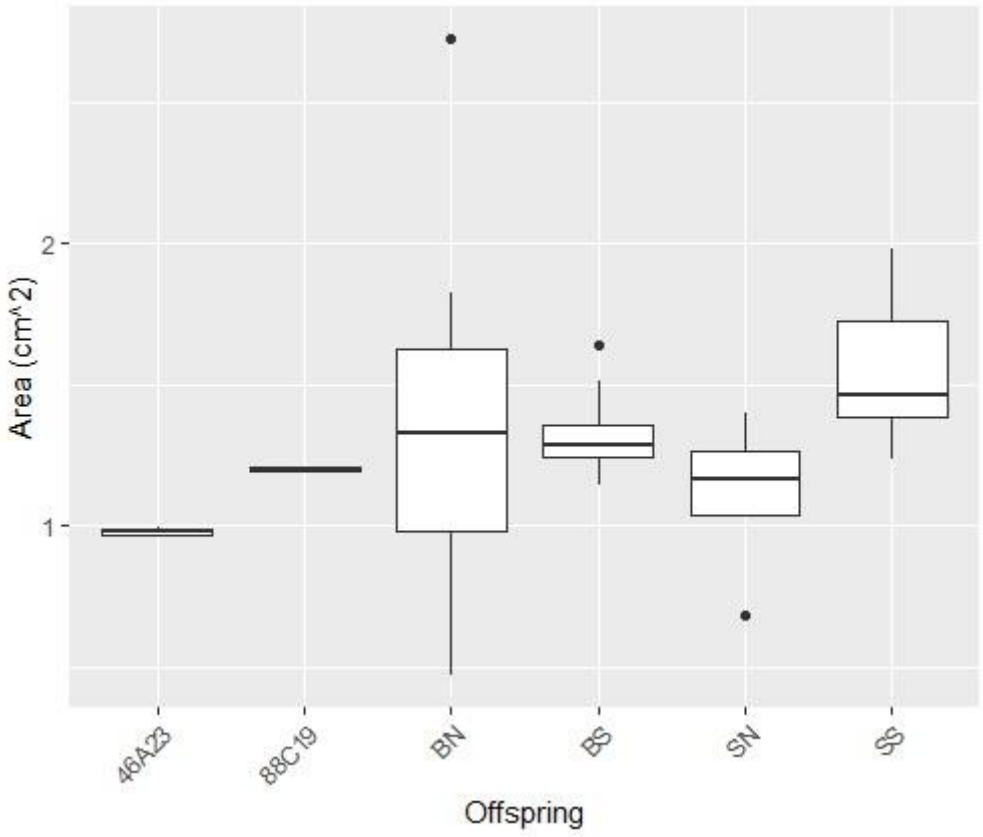

Figure 2: Growth Area of Parental and Offspring Isolates on CM After 48 Hours. *This graph displays the growth areas for 10 measured isolates per phenotype, including the azole-resistant strain 46A23, the azole-sensitive strain 88C19, and the four distinct offspring phenotypes: BN, BS, SN, and SS.*

Initial observations revealed clear phenotypic differences among the offspring. However, these distinctions faded when the isolates were subsequently cultured on individual plates. Figure 2 shows significant variation in growth size across the isolates, with the BN and SN phenotypes generally exhibiting smaller growth areas, whereas the BS and SS phenotypes showed a wider range of growth sizes. Additionally, the parental strains, 46A23 and 88C19, demonstrated distinct growth profiles, with the azole-resistant strain exhibiting more restricted growth compared to the azole-sensitive parental strain.

5.2 Fungicide Susceptibility Test Against Sexual Offspring with Gradient Agar

The resistance profile of the parental isolates against a selection of antifungals was quantitatively assessed using gradient agar plates. These plates were segmented into zones of high and low concentrations for each chemical, as summarized in Table 1. The isolates Afir964, Afir974, and 88C19, which exhibited azole sensitivity, were compared with the azole-resistant isolate 46A23. Antifungal agents showing differential resistance between the parental isolates were selected for further testing against the offspring from the sexual cross of 88C19 and 46A23. This process identified six chemicals of interest for detailed analysis: itraconazole, tebuconazole, benomyl, mancozeb, acriflavine, and azoxystrobin. Results for the latter fungicide are not included in subsequent sections as all offspring, along with isolate 46A23, managed to grow, showing no phenotypic difference among them; refer to Annex 3 for more detail.

Table 1: Antifungal Susceptibility Assessment on Gradient Agar Plates*. This table summarizes the resistance profiles of three azole-sensitive A. fumigatus isolates (AFIR964, AFIR974, and 88C19) and one azole-resistant isolate (46A23) against a selection of twelve antifungal chemicals. Susceptibility was determined by evaluating the isolates' ability to grow and produce spores across gradients of high to low antifungal concentrations. Growth presence, sporulation, and absence of growth were denoted by "+," "++," and "-," respectively.*

		AFIR964		AFIR974		88C19		46A23	
Antifungal	Max Concentration (mg/L)	High Concentration	Low Concentration	High Concentration	Low Concentration	High Concentration	Low Concentration	High Concentration	Low Concentration
Itraconazole	16	-	+	-	+	-	+	++	++
Voriconazole	32	-	+	-	+	-	-	-	+
Posaconazole	2	-	-	-	-	-	-	-	-
Tebuconazole	16	-	+	-	-	-	-	-	+
Azoxystrobin	32	+	++	+	++	-	-	++	++
Benomyl	2	-	+	-	++	-	++	++	++
Propamocarb	32	++	++	++	++	++	++	++	++
Mancozeb	4	-	++	-	++	-	++	++	++
Copper(ii) sulphate 5-hydrate	4	-	++	-	-	-	++	-	++
Copper(ii) sulphate anhydrous	4	-	++	-	-	-	++	-	++
Acriflavine	5	-	+	-	-	-	++	++	++
	20	-	+	-	-	-	++	++	++
Carvacrol	10	-	+	-	-	-	-	-	-
	150	-	+	-	-	-	-	-	-

5.1 Fungicide Susceptibility Test Against Parental and Offspring

In Figure 3, both parental strains 46A23 (azole-resistant) and 88C19 (non-azole-resistant) showed less ability to grow and sporulate than their offspring, with non-azole-resistant parental being less able to grow across treatments. The azole-resistant parental exhibits more growth, both with and without sporulation. The offspring, arising from the cross between these two parental strains, displayed a range of responses to the antifungal treatments. Certain antifungals completely suppressed growth, as indicated by the predominance of blue bars for specific treatments in the analysis. Some treatments permitted growth but prevented sporulation, while a few others allowed both growth and sporulation among the offspring.

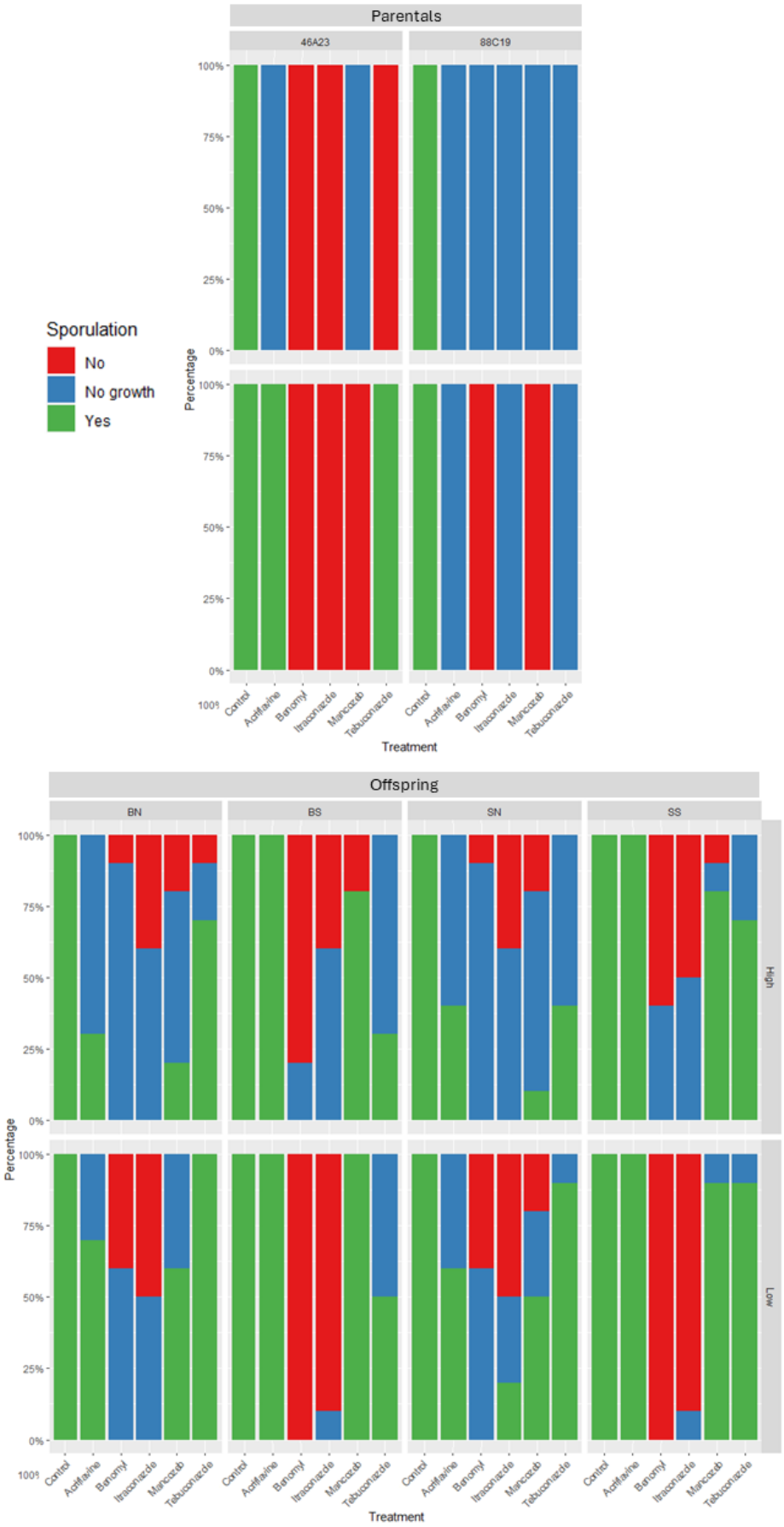
Parentals
46A23
88C19
Sporulation
No
No growth
Yes
Percentage
100%
75%
50%
25%
0%
Control
Acriflavine
Benomyl
Iraconazole
Mancozb
Tebuconazole
Treatment
Offspring
BN
BS
SN
SS
High
Low

Figure 3: Comparative Response of A. fumigatus Parental Strains and Offspring to Antifungal Treatments Based on Growth and Sporulation after 48 hours. *The figure presents the percentage of isolates that were able to grow and sporulate under the influence of different antifungal concentrations. Responses are categorized into three distinct outcomes: growth without sporulation (represented in green), no growth (blue), and growth with sporulation (red).*

Figure 4 indicates the growth area under all treatment conditions was compared to control samples using Wilcoxon tests to determine statistical significance. Both parental strains displayed a reduction in growth area across nearly all treatments. However, an exception was observed with the azole-resistant parental strain (46A23) when exposed to tebuconazole, where the decrease in growth area was not as pronounced. Compared to the parental strains, the offspring demonstrated a wider variation in growth area across treatments. Significant differences in growth area compared to controls were observed in all treatments except for tebuconazole and mancozeb. Also, isolates capable of sporulation generally showed a higher growth area than non-sporulating isolates across all treatments at low concentrations compared to the treatment at high concentrations, except tebuconazole. For tebuconazole, smaller-sized isolates, regardless of their sporulation capacity, exhibited slightly larger growth areas.

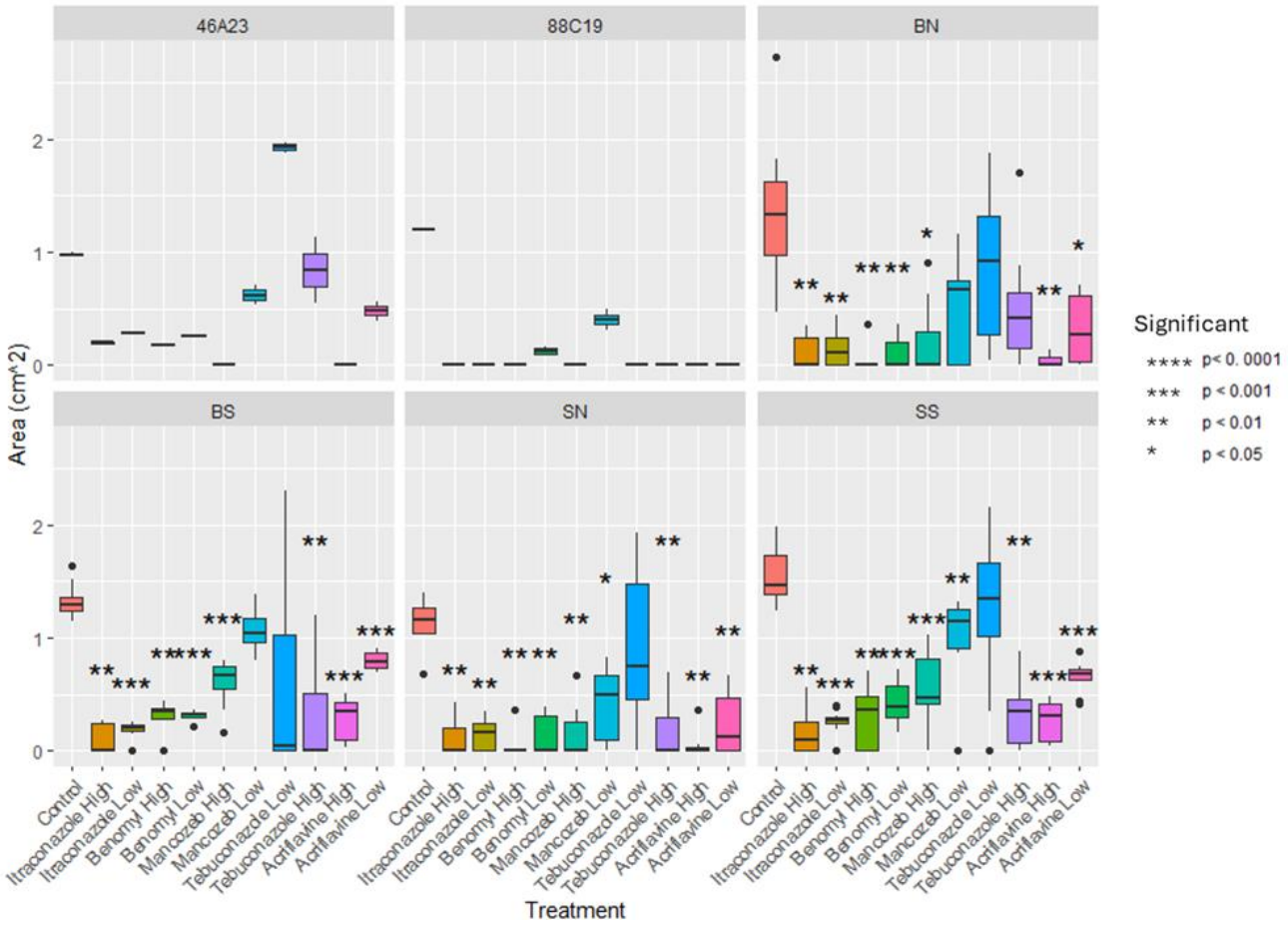

Figure 4: Statistical Evaluation of Antifungal Treatment Effects on A. fumigatus Growth. *This figure displays a statistical analysis comparing the growth of parental A. fumigatus strains and their offspring's phenotypes under various antifungal treatments against control treatments. The analysis employed the Wilcoxon test, with significance levels indicated by asterisks, as defined in the figure's legend.*

Figure 5 uses the same growth area data to further examine the dose-dependent effects of each antifungal treatment on the growth area. A Wilcoxon test was employed to compare growth areas at low and high concentrations for each treatment, shedding light on the concentration-specific responses of the parental strains and their offspring. Significant differences in growth area across all samples were observed for acriflavine and mancozeb, indicating a pronounced dose-dependent response to these treatments.

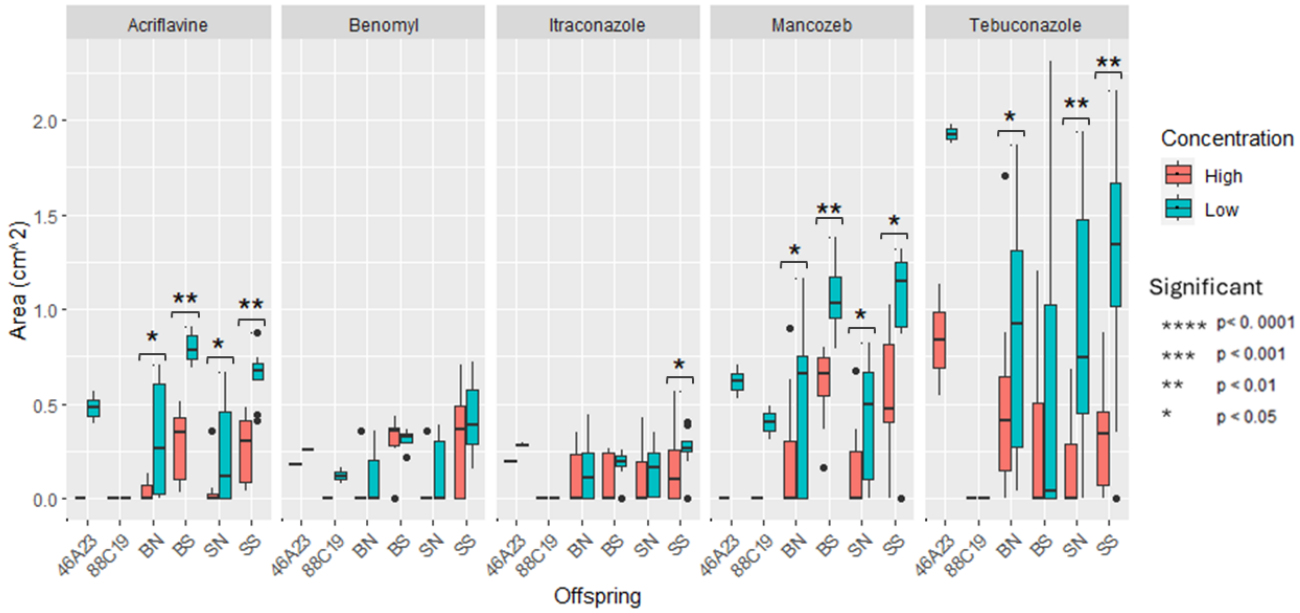

Figure 5: Dose-Dependent Differences in Growth Area Under Antifungal. *This figure illustrates the significant differences in growth area between low and high concentrations of antifungal treatments for both parental strains of A. fumigatus and their phenotypically diverse offspring. Statistical significance was assessed using the Wilcoxon test, with levels of significance denoted by asterisks, as detailed in the figure's legend.*

Figure 6 uses again the same growth area dataset, as in Figures 4 and 5, to present the outcomes of a Kruskal-Wallis test, followed by posthoc Wilcoxon tests for pairwise comparisons, aiming to pinpoint significant growth area differences among all samples under identical antifungal treatment and concentration. This analysis uncovers a broader range of growth area differences among offspring phenotypes compared to the parental strains, particularly in response to acriflavine, benomyl, and mancozeb treatments, where certain phenotypes exhibited notably distinct growth areas.

Furthermore, the analysis indicates that phenotypes BS and SS show a larger growth area in response to non-azole antifungal treatments than azole-based treatments, in contrast to the BN and SN phenotypes and the parental strains. This suggests that certain offspring phenotypes may have a differential sensitivity or resistance pattern to non-azole versus azole antifungals, underlining the complex nature of fungal growth responses to different antifungal classes.

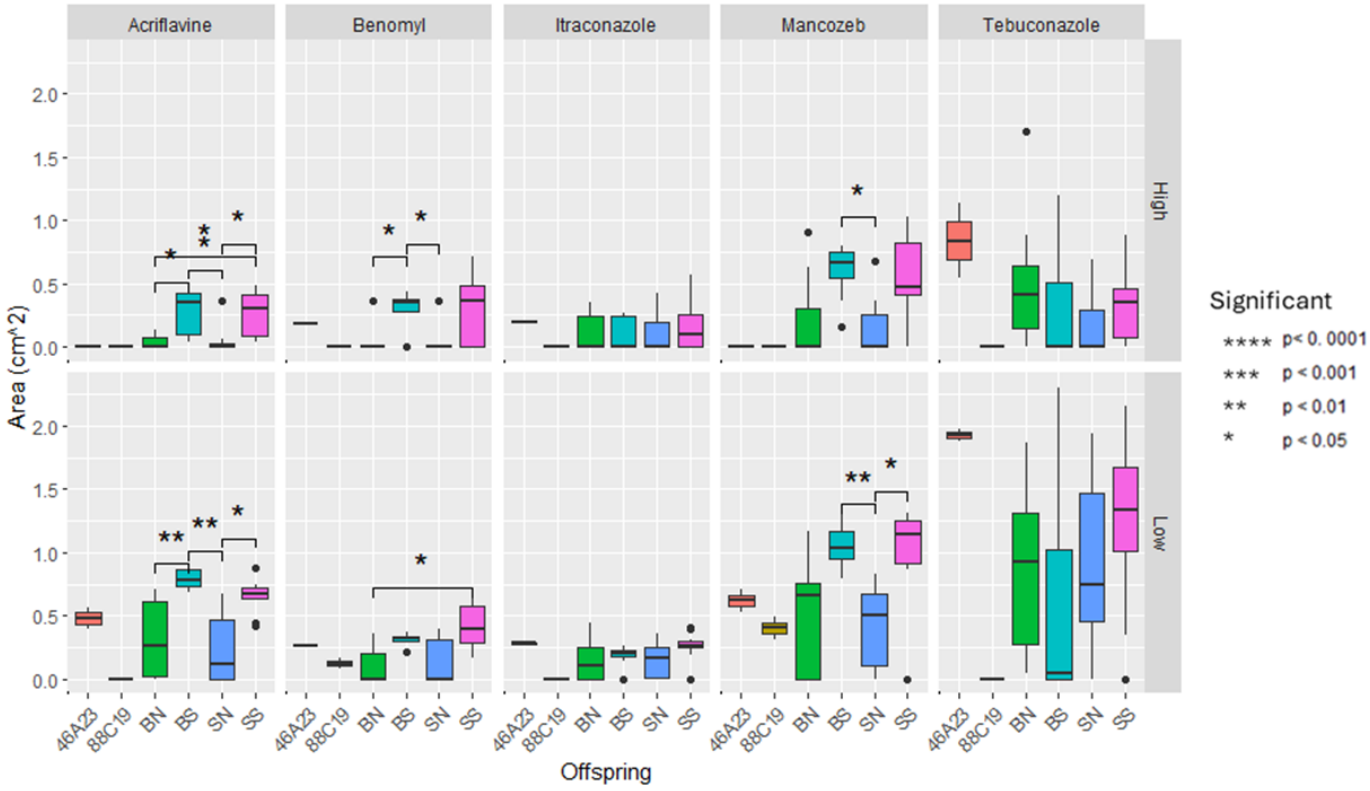

Figure 6: Differential Growth Responses to Antifungal Treatments in A. fumigatus Offspring and Parental Strains*. This figure illustrates the variations in growth area among A. fumigatus offspring phenotypes and parental strains under specific antifungal treatments, emphasizing the distinct resistance profiles against non-azole and azole antifungals. The analysis utilized Kruskal-Wallis and post-hoc Wilcoxon statistical tests. Data are segmented by antifungal type, with unique color coding assigned to offspring phenotypes and parental strains. Statistical significance is indicated by asterisks, with levels of significance detailed in the legend.*

5.2 Quality Control of DNA Samples

Quality control measures confirmed that three samples surpassed the DNA concentration threshold of 20 ng/µL, except for the BN group. Optical density (OD) assessments indicated that all samples, except for BS and BN, had OD 260/230 ratios within the optimal range of 2.0 to 2.2, and OD

260/280 ratios between 1.8 and 2.0, suggesting satisfactory purity. However, an integrity check revealed significant degradation in the SS sample, constraining its suitability for further analysis. The DNA from the BN sample was found to be completely degraded. Detailed results of these assessments are available in Annex 4.

5.3 Bioinformatics Analysis and Gen Identification

To identify QTLs relevant, a QTL-seq analysis was conducted using sequencing data from both Nanopore and Illumina platforms. While the Nanopore dataset did not yield significant findings, notable results were obtained from the Illumina data, which are the focus of this section; detailed Nanopore data are available in Annex 5.

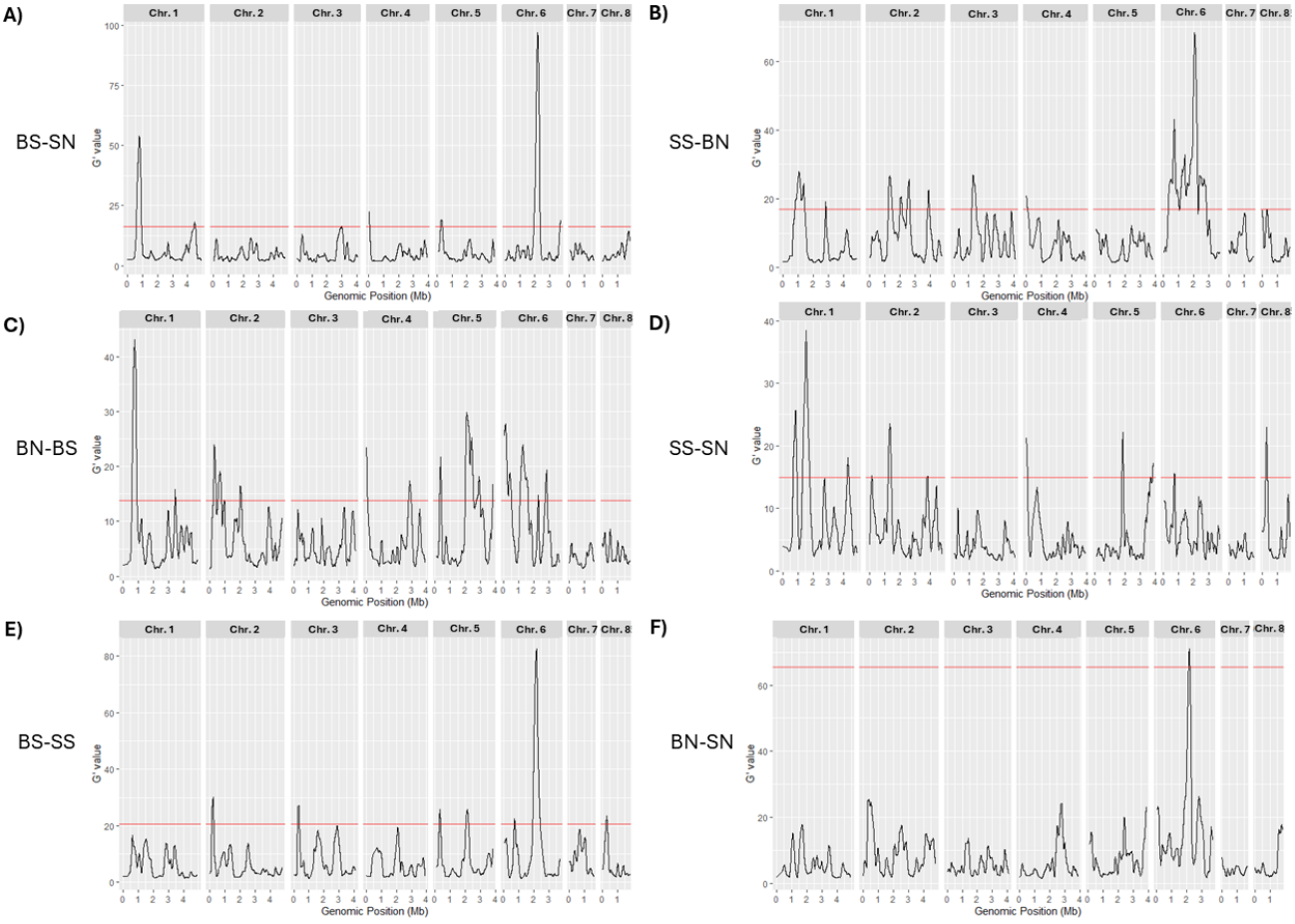

Figure 7: G' values of the significance QTL found between the four different phenotypes identified in C001 using a reference genome Af293. *Significant regions can be identified above the red line (q= 0.001). A) G' values of high bulk SN and low bulk BS. B) G' values of high bulk SS and low bulk BN. C) G' values of high bulk BN and low bulk BS. D) G' values of high bulk SN and low bulk SS. E) G' values of high bulk BS and low bulk SS. F) G' values of high bulk BN and low bulk SN.*

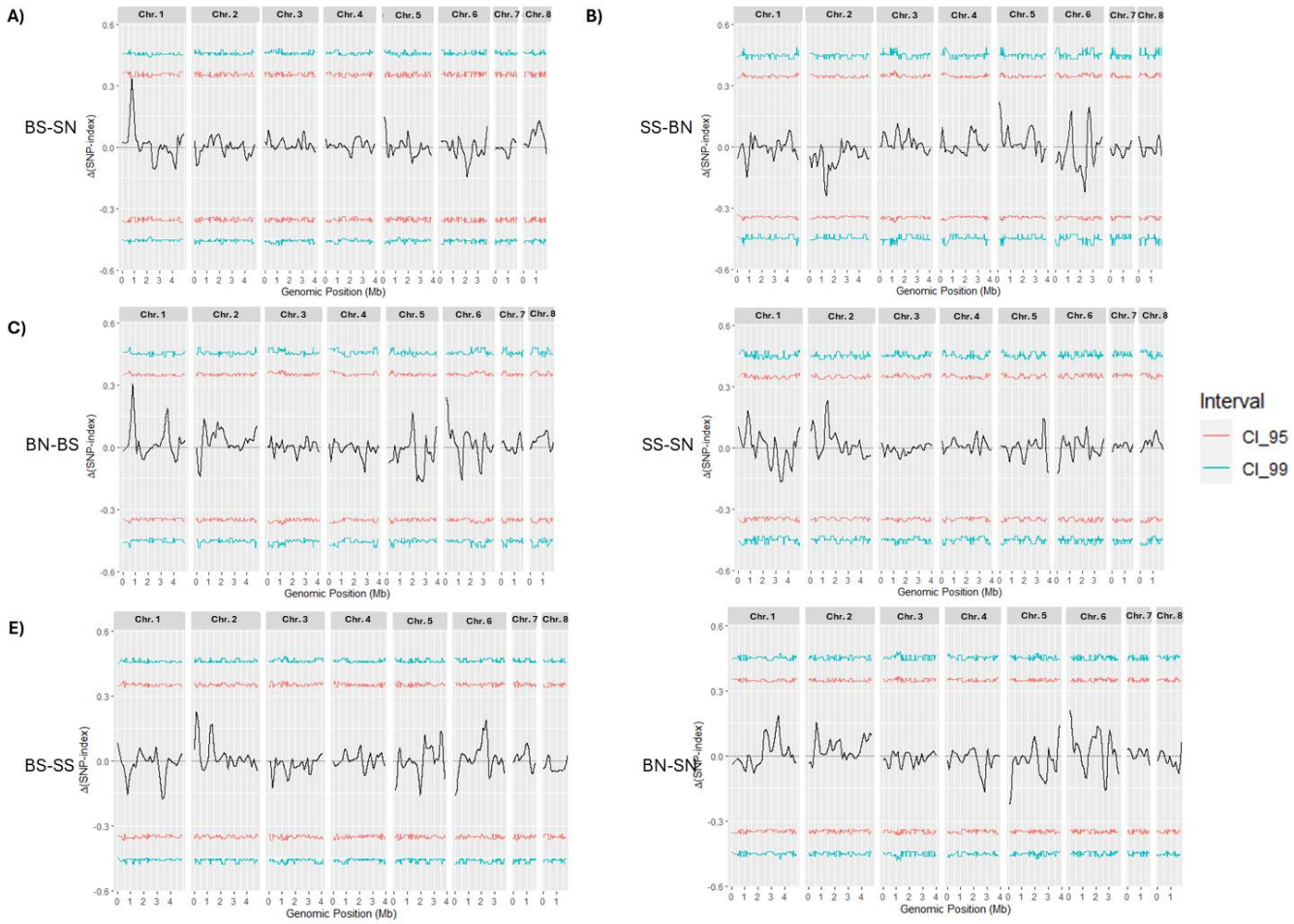

Figure 8: Δ SNP Index Highlighting Significant QTLs Among C001 Offspring Phenotypes Using the Af293 Reference Genome. *This figure illustrates the Δ SNP index values used to identify significant quantitative trait loci (QTL) across the four phenotypes identified in C001. The panels represent comparisons between different phenotype bulks: A) Δ SNP index of high bulk SN and low bulk BS. B) Δ SNP index of high bulk SS and low bulk BN. C) Δ SNP index of high bulk BN and low bulk BS. D) Δ SNP index of high bulk SN and low bulk SS. E) Δ SNP index of high bulk BS and low bulk SS. F) Δ SNP index of high bulk BN and low bulk SN. Significant levels are represented with red and blue lines at 95% and 99% of the level of significance, respectively.*

The analysis of the Illumina dataset highlighted two significant chromosomal regions of interest: the first located on chromosome 1 and the second on chromosome 6, as detailed in the QTL analysis. Figure 7 illustrates significant G' values in these specific genomic regions when isolates with contrasting phenotypes are compared. Notably, chromosome 1 exhibits significant G' values in comparisons between isolates of identical size but differing sporulation capacities, while chromosome 6 reveals significant G' values when comparing isolates that differ in size yet share

similar levels of sporulation. These findings are further corroborated by the ΔSNP-index values presented in Figure 8.

Table 2: Significant QTL Analysis. *This table presents the analysis of significant quantitative trait loci (QTL), detailing for each QTL its number, chromosomal location, start and end points on the chromosome, QTL length, number of single nucleotide polymorphisms (nSNPs), average SNPs (expressed in megabases), average Δ SNP, the position of maximum G' value, and mean G' value. QTLs 1 and 2 are highlighted as the primary areas of interest identified through the analysis.*

QTL	Chromosome	Star	End	Length	nSNPs	Average SNPs (Mb)	Average Delta SNP	Position of max G'prime	Mean G'prime
1	1	539094	950646	411552	755	1835	0,26	768200	41,49
2	6	1898082	2375771	477689	206	431	-0,09	2174496	39,06

Table 3 details the characteristics of the identified QTLs. The QTL on chromosome 1 spans from 539,094 to 950,646 base pairs, with a peak G' value observed at 768,200 base pairs. Conversely, the QTL identified on chromosome 6 extends from 1,898,082 to 2,375,771 base pairs, reaching its highest G' value at 2,174,496 base pairs. Both regions exhibit notably high mean G' values. The ΔSNP index highlights a distinctive pattern between the two regions: chromosome 1 shows an increase in SNP density towards the end of the QTL, whereas chromosome 6 displays a lower SNP quantity and reduced read numbers in specific QTL regions, as detailed in Annex 6.

The substantial QTL on chromosome 1 contains a dense cluster of SNPs surrounding various genes. Significant genes located within approximately 10,000 base pairs of the peak G' value include rRNA processing proteins (AFUA_1G02610 and AFUA_1G02636), tRNA-Asp genes (AFUA_1G02633 and AFUA_1G02636), a gene with a PPM-type phosphatase-like domain (AFUA_1G02640), a gene with a C6 finger domain (AFUA_1G02650), and an F-Box domain protein (AFUA_1G02660). The QTL on chromosome 6, characterized by fewer SNPs and areas with sparse read coverage, suggests potential structural variations that might impact SNP density in this region.

6 Discussion

The emerging resistance of *A. fumigatus* to not only azoles but also to a broader range of fungicides utilized in agricultural settings represents a significant public health concern, particularly regarding the future development of aspergillosis treatments (Hahn, 2014; Sofianos et al., 2023). Despite considerable research efforts focused on azole resistance, the understanding of the mechanisms conferring resistance to a wider spectrum of fungicides remains limited (Fraaije et al., 2020; Gonzalez-Jimenez et al., 2021; Kang et al., 2022). To address this knowledge gap, the investigation should focus on identifying the resistance patterns of *A. fumigatus* to non-azole

fungicides and explore its correlations with the fungus's known resistant genes. The significance of understanding these genetic correlations lies in its potential to guide the identification of novel, effective treatments for aspergillosis, specifically by targeting antifungal agents that can bypass this new resistance pathway.

Building upon this foundation, this research used sexual crosses between the azole-resistant strain (46A23) and the azole-susceptible strain (88C19). Employing sexual reproduction as a base methodology for the research marks a significant departure from traditional approaches that often rely on asexual reproduction or exhibit limited genetic diversity. This innovative approach facilitates the creation of offspring exhibiting a wide range of phenotypical variations, thereby helping in the identification of relevant traits and the genes responsible for them (Kück et al., 2022). Coupling BSA with next-generation sequencing enables to pinpointing genes associated with specific phenotypes of interest, like fungicide resistance (Ashton et al., 2022). Recent studies further emphasize the relevance of this approach, proposing that sexual reproduction in *A. fumigatus* might be more prevalent in natural environments than previously assumed (Zhang et al., 2022). This finding suggests that, similarly to azole resistance, the emergence of resistance to other fungicides in *A. fumigatus* could also emerge through this process (Zhang et al., 2020).

To detect potential resistance patterns, susceptibility tests against a selection of fungicidal chemicals were conducted. These tests revealed distinct growth patterns between the parental strains. While 88C19 remained susceptible to most antifungals, it exhibited some growth at low concentrations of mancozeb and benomyl. In contrast, the azole-resistant parent, 46A23, exhibited robust growth across itraconazole, tebuconazole, benomyl, mancozeb, acriflavine, and azoxystrobin treatments with a slight effect on sporulation for some of these chemicals. This reduction in sporulation at higher antifungal concentrations reflects a dose-dependent response to each fungicide, aligning with expects response of fungi under stress conditions (Van den Bosch et al., 2011). It is not unexpected to find the 46A23 strain resistant not only to azoles but also to other antifungal agents—a pattern that has been documented in certain *A. fumigatus* isolates (Fraaije et al., 2020; Fraaije et al., 2021; Meneau & Sanglard, 2005), and has also been described across various human-pathogenic fungi (Lucas et al., 2015). The development of resistance to multiple fungicides in fungi, mirroring antibiotic resistance in bacteria, suggests an evolutionary trend towards accumulating resistance alleles against non-azole fungicides due to environmental pressures (Kang et al., 2022).

Among the offspring, distinct resistance profiles emerged, highlighting a heritable and phenotype-specific response to azole versus non-azole fungicide, with the clear exception of azoxystrobin. Offspring capable of sporulation (BS and SS) exhibited enhanced resistance to non-azole fungicides compared to their non-sporulating counterparts (BN and SN). This finding challenges the conventional belief that resistance acquisition leads to fitness costs, such as reduced size or the absence of sporulation compared to wild-type isolates (Hawkins & Fraaije, 2018; Manners & Dodd, 2019). This discrepancy suggests that the resistance mechanisms may not be fungicide-

specific but rather involve broader genetic adaptations, possibly related to quantitative resistance to fungicides (Deising et al., 2008). Such adaptations might explain the varied resistance levels observed among isolates with the same phenotypes and highlight the complexity of fungicide resistance mechanisms. These range from disrupting ergosterol biosynthesis in the case of itraconazole and tebuconazole, to direct impacts of benomyl, mancozeb, and acriflavine on fungal cells (FRAC, 2023). This diversity in resistance mechanisms likely results from different genes being involved in the regulation or expression of multidrug efflux pumps, indicating a complex genetic basis for the observed resistance patterns (Gikas et al., 2022; Hu & Chen, 2021; Pereira et al., 2020). In the case of azoxystrobin, no distinct pattern was observed. All offspring and the azole-resistant parental strain grew without issue, unlike the non-azole-resistant parental strain. This is not surprising since azoxystrobin, a fungicide that affects mitochondrial respiration, is commonly used alongside azole fungicides, meaning that mutations in *cytB*, which confer resistance to azoxystrobin, are often found in such isolates (Jørgensen et al., 2021; Oliveira et al., 2022). If the offspring inherited their mitochondria from the azole-resistant parent, they also inherit resistance to azoxystrobin (Zhao et al., 2009).

Building upon these findings, identifying potential genes responsible for the observed resistance patterns became a priority. Given the phenotypic contrasts among the offspring, segregant isolates were selected for BSA analysis. initial attempts with nanopore sequencing offered quick insights but failed to yield significant G' values or ΔSNP indexes, likely due to its higher base-level error rate compared to the more accurate, even though slower, Illumina sequencing (Shafin et al., 2021).

The significant QTL identified by Snelders et al. (unpublished) in chromosome 5 was not identified with this analysis. However, with the Illumina sequencing two significant QTLs on chromosomes 1 and 6 were identified. Interestingly, the presence of each QTL was limited upon specific BSA comparisons, either based on sporulation capabilities or size differences among the isolates. Consequently, the QTL on chromosome 1 was exclusively identified in comparisons between offspring with varying sporulation capacities, such as BS with BN or SS with SN. Meanwhile, the QTL on chromosome 6 emerged in comparisons focusing on growth area differences among the offspring, such as BS with SS or BN with SN. Considering the established correlation between sporulation and resistance to non-azole fungicides (benomyl, mancozeb, and acriflavine), the QTL identified on chromosome 1 might also relate to resistance traits.

As such the focus on the QTL found on chromosome 1 relies on identifying what may cause the changes in sporulation and resistance to the non-azole fungicides tested, determining if both characteristics are caused by the same mechanism. An effective initial strategy involves identifying potential genes near the highest G' values and relevant SNPs (Li & Xu, 2022). Consequently, genes proximate to these markers include rRNA processing proteins (AFUA_1G02610 and AFUA_1G02636), tRNA-Asp (AFUA_1G02633 and AFUA_1G02636), a gene with a PPM-type phosphatase-like domain (AFUA_1G02640), a gene with a C6 finger domain (AFUA_1G02650), and an F-Box domain protein (AFUA_1G02660). Determining the direct impact of these genes on

sporulation, resistance, or both presents a considerable challenge. Current insights into antifungal resistance mechanisms, such as alterations or overexpression of drug targets and mutations in critical genes like ERG11 and FKS, do not directly link these resistance pathways to the genes of interest or their effects on fungal sporulation (Lee et al., 2023).

In contrast, the fewer SNPs observed in the QTL on chromosome 6 hint at possible structural variations, such as mobile elements (Zhang & Panthee, 2022). This theory becomes particularly convincing upon examining regions near the highest G' value, which exhibit notably low or absent read numbers relative to the reference genome. This QTL is proximal to a genomic section characterized by an unusual composition, including various transposons, such as gypsy, LINE, and TY1Copia, transposon fragments, pseudogenes, and genes horizontally transferred from other eukaryotic organisms (Mallet et al., 2010).

The complexity of identifying QTLs is intensified by reports of significant chromosomal deletions in chromosomes 1 and 6, as documented by several studies (Abdolrasouli et al., 2015; Garcia-Rubio et al., 2018; Puértolas-Balint et al., 2019). These deletions can alter the genetic landscape around the QTLs, potentially impacting traits associated with resistance, sporulation, and growth. Deletions on chromosome 1 extend up to 491 kb from its benign end, while chromosome 6 exhibits a deletion of approximately 2267 kb. Despite the QTL on chromosome 1 not directly overlapping with these deletions, it may still be indirectly influenced by the resultant genomic alterations or shifts in the genetic context. Meanwhile, the QTL on chromosome 6, especially within the region experiencing reduced read counts between 2214 kb and 2386 kb, overlaps with these deletions, suggesting that a potential structural variation or disruption may be linked to the trait of interest. Moreover, rearrangements reported in chromosomes 1 and 6, despite unspecified locations, could also affect the identified QTLs (Bowyer et al., 2022).

The study's innovative methodologies, including sexual crosses and BSA, have unveiled significant variations in resistance profiles among parental strains and their offspring, challenging conventional assumptions about fungicide resistance in *A. fumigatus*. Two significant QTLs on chromosomes 1 and 6, we uncovered. These genomic regions, particularly the identified candidate genes associated with growth size and sporulation, offer promising avenues for further research into the molecular mechanisms underlying resistance traits. Moreover, the presence of structural variations near the QTL on chromosome 6, such as transposons and horizontally transferred genes, highlights the genetic complexity that may affect the traits of interest. While these findings are significant, they come with limitations due to the dependence on particular strains, a constrained sample size, and the specific conditions of laboratory studies. These factors may limit the broader applicability of the results. Broadening the scope to include a more diverse array of fungal strains and using alternative sequencing technologies could address some of these limitations. Additionally, the potential application of CRISPR-Cas9 technology for functional genomics research offers an exciting avenue for clarifying the roles of candidate genes in resistance

mechanisms. This could involve generating specific gene knockouts, knockdowns, or modifications to elucidate their direct contributions to fungicide resistance.

7 Conclusions & Recommendations

The revelation of genetic mechanisms behind *A. fumigatus* resistance to a broad spectrum of fungicides. The identification of critical quantitative trait loci on chromosomes 1 and 6 offers a new lens through which to view resistance, extending beyond azoles to encompass multi-drug resistance. These findings are the first analysis to fill the gap in our knowledge regarding the genetic basis of non-azole resistance in *A. fumigatus*, which is vital for developing future aspergillosis treatment strategies capable of avoiding such resistance.

Future studies should aim to increase the knowledge of the genetic diversity of the *A. fumigatus* strains related to non-azole resistance. An expanded approach that incorporates both clinical isolates and environmental samples will enrich our understanding of resistance mechanisms. Clinical isolates will shed light on resistance encountered in human infections, whereas environmental samples can unveil naturally occurring resistance patterns, potentially induced by the use of agricultural fungicides. Given the complexity of this topic, a comprehensive approach that merges genotypic, phenotypic, and environmental analyses is recommended. Advancements in sequencing technologies and the application of functional genomics approaches, like CRISPR-Cas9 editing, are recommended to dissect the roles of candidate genes within the identified QTLs on chromosomes 1 and 6. Targeted gene modifications, including knockouts, knockdowns, or insertion mutations, will allow for direct observation of their effects on fungicide resistance and other phenotypically relevant traits. Specifically, editing genes within the QTL on chromosome 1 could clarify their roles in sporulation and resistance to non-azole fungicides, while modifications in the QTL on chromosome 6 could help interpret the impact of growth sizes and transposable elements on resistance profiles.

8 References

Abdolrasouli, A., Rhodes, J., Beale, M. A., Hagen, F., Rogers, T. R., Chowdhary, A., Meis, J. F., Armstrong-James, D., & Fisher, M. C. (2015). Genomic Context of Azole Resistance Mutations in Aspergillus fumigatus Determined Using Whole-Genome Sequencing. *MBio*, *6*(3). https://doi.org/10.1128/MBIO.00536-15

Anderson, J. B. (2005). Evolution of antifungal-drug resistance: mechanisms and pathogen fitness. *Nature Reviews Microbiology 2005 3:7*, *3*(7), 547–556. https://doi.org/10.1038/nrmicro1179

Ashton, G. D., & Dyer, P. S. (2019). Culturing and Mating of Aspergillus fumigatus. *Current Protocols in Microbiology*, *54*(1). https://doi.org/10.1002/CPMC.87

Ashton, G. D., Sang, F., Blythe, M., Zadik, D., Holmes, N., Malla, S., Camps, S. M. T., Wright, V., Melchers, W. J. G., Verweij, P. E., & Dyer, P. S. (2022). Use of Bulk Segregant Analysis for Determining the Genetic Basis of Azole Resistance in the Opportunistic Pathogen Aspergillus fumigatus. *Frontiers in Cellular and Infection Microbiology*, *12*, 841138. https://doi.org/10.3389/FCIMB.2022.841138/BIBTEX

Assress, H. A., Selvarajan, R., Nyoni, H., Mamba, B. B., & Msagati, T. A. M. (2021). Antifungal azoles and azole resistance in the environment: current status and future perspectives—a review. *Reviews in Environmental Science and Bio/Technology 2021 20:4*, *20*(4), 1011–1041. https://doi.org/10.1007/S11157-021-09594-W

Auxier, B., Debets, A. J. M., Stanford, F. A., Rhodes, J., Becker, F. M., Marquez, F. R., Nijland, R., Dyer, P. S., Fisher, M. C., den Heuvel, J. van, & Snelders, E. (2023). The human fungal pathogen Aspergillus fumigatus can produce the highest known number of meiotic crossovers. *PLOS Biology*, *21*(9), e3002278. https://doi.org/10.1371/JOURNAL.PBIO.3002278

Bastos, R. W., Rossato, L., Goldman, G. H., & Santos, D. A. (2021). Fungicide effects on human fungal pathogens: Cross-resistance to medical drugs and beyond. *PLoS Pathogens*, *17*(12). https://doi.org/10.1371/JOURNAL.PPAT.1010073

Berger, S., Chazli, Y. El, Babu, A. F., & Coste, A. T. (2017). Azole resistance in Aspergillus fumigatus: A consequence of antifungal use in agriculture? *Frontiers in Microbiology*, *8*(JUN), 265517. https://doi.org/10.3389/FMICB.2017.01024

Bongomin, F., Gago, S., Oladele, R. O., & Denning, D. W. (2017). Global and Multi-National Prevalence of Fungal Diseases—Estimate Precision. *Journal of Fungi 2017, Vol. 3, Page 57*, *3*(4), 57. https://doi.org/10.3390/JOF3040057

Bowyer, P., Currin, A., Delneri, D., & Fraczek, M. G. (2022). Telomere-to-telomere genome sequence of the model mold pathogen Aspergillus fumigatus. *Nature Communications 2022 13:1*, *13*(1), 1–7. https://doi.org/10.1038/s41467-022-32924-7

Brauer, V. S., Rezende, C. P., Pessoni, A. M., De Paula, R. G., Rangappa, K. S., Nayaka, S. C., Gupta, V. K., & Almeida, F. (2019). Antifungal Agents in Agriculture: Friends and Foes of Public Health. *Biomolecules*, *9*(10). https://doi.org/10.3390/BIOM9100521

Deising, H. B., Reimann, S., & Pascholati, S. F. (2008). Mechanisms and significance of fungicide resistance. *Brazilian Journal of Microbiology*, *39*(2), 286. https://doi.org/10.1590/S1517-838220080002000017

Fraaije, B. A., Atkins, S. L., Santos, R. F., Hanley, S. J., West, J. S., & Lucas, J. A. (2021). Epidemiological studies of pan-azole resistant aspergillus fumigatus populations sampled during tulip cultivation show clonal expansion with the acquisition of multi-fungicide resistance as a potential driver. *Microorganisms*, *9*(11), 2379. https://doi.org/10.3390/MICROORGANISMS9112379/S1

Fraaije, B., Atkins, S., Hanley, S., Macdonald, A., & Lucas, J. (2020). The Multi-Fungicide Resistance Status of Aspergillus fumigatus Populations in Arable Soils and the Wider European Environment. *Frontiers in Microbiology*, *11*, 599233. https://doi.org/10.3389/FMICB.2020.599233

FRAC. (2023). *FRAC Code List ©* 2023: Fungal control agents sorted by cross-resistance pattern and mode of action (including coding for FRAC Groups on product labels)*. https://www.frac.info/docs/default-source/publications/frac-code-list/frac-code-list-2023---final.pdf

Garcia-Rubio, R., Monzon, S., Alcazar-Fuoli, L., Cuesta, I., & Mellado, E. (2018). Genome-Wide Comparative Analysis of Aspergillus fumigatus Strains: The Reference Genome as a Matter of Concern. *Genes*, *9*(7). https://doi.org/10.3390/GENES9070363

Gikas, G. D., Parlakidis, P., Mavropoulos, T., & Vryzas, Z. (2022). Particularities of Fungicides and Factors Affecting Their Fate and Removal Efficacy: A Review. *Sustainability 2022, Vol. 14, Page 4056*, *14*(7), 4056. https://doi.org/10.3390/SU14074056

Gonzalez-Jimenez, I., Garcia-Rubio, R., Monzon, S., Lucio, J., Cuesta, I., & Mellado, E. (2021). Multiresistance to nonazole fungicides in aspergillus fumigatus TR34/L98H Azole-resistant isolates. *Antimicrobial Agents and Chemotherapy*, *65*(9). https://doi.org/10.1128/AAC.00642-21

Gonzalez-Jimenez, I., Lucio, J., Amich, J., Cuesta, I., Arroyo, R. S., Alcazar-Fuoli, L., & Mellado, E. (2020). A Cyp51B Mutation Contributes to Azole Resistance in Aspergillus fumigatus. *Journal of Fungi*, *6*(4), 1–16. https://doi.org/10.3390/JOF6040315

Greeff, S. de, & Mouton, J. (2017). *NethMap 2017: Consumption of antimicrobial agents and antimicrobial resistance among medically important bacteria in the Netherlands / MARAN 2017: Monitoring of antimicrobial resistance and antibiotic usage in animals in the Netherlands in 2016*. https://doi.org/10.21945/RIVM-2017-0056

Guinea, J., Verweij, P. E., Meletiadis, J., Mouton, J. W., Barchiesi, F., Arendrup, M. C., Arikan-Akdagli, S., Castanheira, M., Chryssanthou, E., Friberg, N., Järv, H., Klimko, N., Kurzai,

O., Lagrou, K., Lass-Flörl, C., Mares, M., Matos, T., Moore, C. B., Muehlethaler, K., … Velegraki, A. (2019). How to: EUCAST recommendations on the screening procedure E.Def 10.1 for the detection of azole resistance in Aspergillus fumigatus isolates using four-well azole-containing agar plates. *Clinical Microbiology and Infection*, *25*(6), 681–687. https://doi.org/10.1016/j.cmi.2018.09.008

Hagiwara, D., Watanabe, A., Kamei, K., & Goldman, G. H. (2016). Epidemiological and genomic landscape of azole resistance mechanisms in Aspergillus fungi. *Frontiers in Microbiology*, *7*(SEP), 214993. https://doi.org/10.3389/FMICB.2016.01382

Hahn, M. (2014). The rising threat of fungicide resistance in plant pathogenic fungi: Botrytis as a case study. *Journal of Chemical Biology*, *7*(4), 133–141. https://doi.org/10.1007/S12154-014-0113-1

Hawkins, N. J., & Fraaije, B. A. (2018). Fitness Penalties in the Evolution of Fungicide Resistance. *Https://Doi.Org/10.1146/Annurev-Phyto-080417-050012*, *56*, 339–360. https://doi.org/10.1146/ANNUREV-PHYTO-080417-050012

Hu, M., & Chen, S. (2021). Non-Target Site Mechanisms of Fungicide Resistance in Crop Pathogens: A Review. *Microorganisms*, *9*(3), 1–19. https://doi.org/10.3390/MICROORGANISMS9030502

Jørgensen, K. M., Helleberg, M., Hare, R. K., Jørgensen, L. N., & Arendrup, M. C. (2021). Dissection of the Activity of Agricultural Fungicides against Clinical Aspergillus Isolates with and without Environmentally and Medically Induced Azole Resistance. *Journal of Fungi*, *7*(3), 205. https://doi.org/10.3390/JOF7030205

Kang, S. E., Sumabat, L. G., Melie, T., Mangum, B., Momany, M., & Brewer, M. T. (2022). Evidence for the agricultural origin of resistance to multiple antimicrobials in Aspergillus fumigatus, a fungal pathogen of humans. *G3 Genes|Genomes|Genetics*, *12*(2). https://doi.org/10.1093/G3JOURNAL/JKAB427

Khateb, A., Gago, S., Bromley, M., Richardson, M., & Bowyer, P. (2023). Aneuploidy Is Associated with Azole Resistance in Aspergillus fumigatus. *Antimicrobial Agents and Chemotherapy*, *67*(4). https://doi.org/10.1128/AAC.01253-22

Kocić-Tanackov, S., Dimić, G., Tanackov, I., Pejin, D., Mojović, L., & Pejin, J. (2012). The inhibitory effect of oregano extract on the growth of Aspergillus spp. and sterigmatocystin biosynthesis. *LWT*, *49*(1), 14–20. https://doi.org/10.1016/J.LWT.2012.04.013

Kück, U., Bennett, R. J., Wang, L., & Dyer, P. S. (2022). Editorial: Sexual and Parasexual Reproduction of Human Fungal Pathogens. *Frontiers in Cellular and Infection Microbiology*, *12*. https://doi.org/10.3389/FCIMB.2022.934267

Lee, Y., Robbins, N., & Cowen, L. E. (2023). Molecular mechanisms governing antifungal drug resistance. *Npj Antimicrobials and Resistance 2023 1:1*, *1*(1), 1–9. https://doi.org/10.1038/s44259-023-00007-2

Lestrade, P. P. A., Buil, J. B., Van Der Beek, M. T., Kuijper, E. J., Dijk, K. Van, Kampinga, G. A., Rijnders, B. J. A., Vonk, A. G., De Greeff, S. C., Schoffelen, A. F., Dissel, J. Van, Meis, J. F., Melchers, W. J. G., & Verweij, P. E. (2020). Paradoxal Trends in Azole-Resistant Aspergillus fumigatus in a National Multicenter Surveillance Program, the Netherlands, 2013–2018 - Volume 26, Number 7—July 2020 - Emerging Infectious Diseases journal - CDC. *Emerging Infectious Diseases*, *26*(7), 1447–1455. https://doi.org/10.3201/EID2607.200088

Li, Z., & Xu, Y. (2022). Bulk segregation analysis in the NGS era: a review of its teenage years. *The Plant Journal*, *109*(6), 1355–1374. https://doi.org/10.1111/TPJ.15646

Lucas, J. A., Hawkins, N. J., & Fraaije, B. A. (2015). The Evolution of Fungicide Resistance. *Advances in Applied Microbiology*, *90*, 29–92. https://doi.org/10.1016/BS.AAMBS.2014.09.001

MacEdo, D., Devoto, T. B., Pola, S., Finquelievich, J. L., Cuesta, M. L., & Garcia-Effron, G. (2020). A Novel Combination of CYP51A Mutations Confers Pan-Azole Resistance in Aspergillus fumigatus. *Antimicrobial Agents and Chemotherapy*, *64*(8). https://doi.org/10.1128/AAC.02501-19

Mallet, L. V., Becq, J., & Deschavanne, P. (2010). Whole genome evaluation of horizontal transfers in the pathogenic fungus Aspergillus fumigatus. *BMC Genomics*, *11*(1), 171. https://doi.org/10.1186/1471-2164-11-171

Manners, A., & Dodd, S. (2019). *Nursery levy at work: Fungicides, Resistance and their Management in Production Nurseries Fungicides, Resistance and their Management in Production Nurseries*.

Meneau, I., & Sanglard, D. (2005). Azole and fungicide resistance in clinical and environmental Aspergillus fumigatus isolates. *Medical Mycology*, *43*(SUPPL.1), S307–S311. https://doi.org/10.1080/13693780500090826/2/13693780500090826FIG001.JPEG

Mikaberidze, A., & McDonald, B. A. (2015). Fitness Cost of Resistance: Impact on Management. *Fungicide Resistance in Plant Pathogens*, 77–89. https://doi.org/10.1007/978-4-431-55642-8_6

Oliveira, T. Y. K., Silva, T. C., Moreira, S. I., Christiano, F. S., Gasparoto, M. C. G., Fraaije, B. A., & Ceresini, P. C. (2022). Evidence of Resistance to QoI Fungicides in Contemporary Populations of Mycosphaerella fijiensis, M. musicola, and M. thailandica from Banana Plantations in Southeastern Brazil. *Agronomy 2022, Vol. 12, Page 2952*, *12*(12), 2952. https://doi.org/10.3390/AGRONOMY12122952

O'Gorman, C. M., Fuller, H. T., & Dyer, P. S. (2009). Discovery of a sexual cycle in the opportunistic fungal pathogen Aspergillus fumigatus. *Nature 2009 457:7228*, *457*(7228), 471–474. https://doi.org/10.1038/nature07528

Pereira, D., McDonald, B. A., & Croll, D. (2020). The Genetic Architecture of Emerging Fungicide Resistance in Populations of a Global Wheat Pathogen. *Genome Biology and Evolution*, *12*(12), 2231. https://doi.org/10.1093/GBE/EVAA203

Piprotar, J. G., Kanzaria, K. K., Zankat, R. M., & Kelaiya, D. S. (2022). Evaluation of fungicides against Aspergillus niger van Tieghem causing collar rot of groundnut under laboratory and field condition. *The Pharma Innovation Journal*, *11*(9), 2285–2291. www.thepharmajournal.com

Puértolas-Balint, F., Rossen, J. W. A., Oliveira dos Santos, C., Chlebowicz, M. M. A., Raangs, E. C., van Putten, M. L., Sola-Campoy, P. J., Han, L., Schmidt, M., & García-Cobos, S. (2019). Revealing the Virulence Potential of Clinical and Environmental Aspergillus fumigatus Isolates Using Whole-Genome Sequencing. *Frontiers in Microbiology*, *10*. https://doi.org/10.3389/FMICB.2019.01970/FULL

Rhodes, J., Abdolrasouli, A., Dunne, K., Sewell, T. R., Zhang, Y., Ballard, E., Brackin, A. P., van Rhijn, N., Chown, H., Tsitsopoulou, A., Posso, R. B., Chotirmall, S. H., McElvaney, N. G., Murphy, P. G., Talento, A. F., Renwick, J., Dyer, P. S., Szekely, A., Bowyer, P., … Fisher, M. C. (2022). Population genomics confirms acquisition of drug-resistant Aspergillus fumigatus infection by humans from the environment. *Nature Microbiology 2022 7:5*, *7*(5), 663–674. https://doi.org/10.1038/s41564-022-01091-2

Schoustra, S. E., Debets, A. J. M., Rijs, A. J. M. M., Zhang, J., Snelders, E., Leendertse, P. C., Melchers, W. J. G., Rietveld, A. G., Zwaan, B. J., & Verweij, P. E. (2019). Environmental Hotspots for Azole Resistance Selection of Aspergillus fumigatus, the Netherlands. *Emerging Infectious Diseases*, *25*(7), 1347. https://doi.org/10.3201/EID2507.181625

Shafin, K., Pesout, T., Chang, P. C., Nattestad, M., Kolesnikov, A., Goel, S., Baid, G., Kolmogorov, M., Eizenga, J. M., Miga, K. H., Carnevali, P., Jain, M., Carroll, A., & Paten, B. (2021). Haplotype-aware variant calling with PEPPER-Margin-DeepVariant enables high accuracy in nanopore long-reads. *Nature Methods 2021 18:11*, *18*(11), 1322–1332. https://doi.org/10.1038/s41592-021-01299-w

Snelders, E., Celia-Sanchez, B. N., Nederlof, Y., Zhang, J., Kortenbosch, H., Kooreman-Tehupeiory, M., Wang, L., Van Dijk, K., Brewer, M. T., Momany, M., Zwaan, B. J., Auxier, B., & Verweij, P. E. (unpublished.). *Widely dispersed clonal expansion of multi fungicide resistant Aspergillus fumigatus limits genomic 1 epidemiology prospects 2 3*.

Sofianos, G., Samaras, A., & Karaoglanidis, G. (2023). Multiple and multidrug resistance in Botrytis cinerea: molecular mechanisms of MLR/MDR strains in Greece and effects of co-existence of different resistance mechanisms on fungicide sensitivity. *Frontiers in Plant Science*, *14*, 1273193. https://doi.org/10.3389/FPLS.2023.1273193/BIBTEX

Song, J., Li, R., & Jiang, J. (2019). Copper Homeostasis in Aspergillus fumigatus: Opportunities for Therapeutic Development. *Frontiers in Microbiology*, *10*(APR). https://doi.org/10.3389/FMICB.2019.00774

Van De Veerdonk, F. L., Gresnigt, M. S., Romani, L., Netea, M. G., & Latgé, J. P. (2017). Aspergillus fumigatus morphology and dynamic host interactions. *Nature Reviews Microbiology 2017 15:11*, *15*(11), 661–674. https://doi.org/10.1038/nrmicro.2017.90

Van den Bosch, F., Paveley, N., Shaw, M., Hobbelen, P., & Oliver, R. (2011). The dose rate debate: does the risk of fungicide resistance increase or decrease with dose? *Plant Pathology*, *60*(4), 597–606. https://doi.org/10.1111/J.1365-3059.2011.02439.X

Zhang, J., Debets, A. J. M., Verweij, P. E., & Snelders, E. (2021). Azole-Resistance Development; How the Aspergillus fumigatus Lifecycle Defines the Potential for Adaptation. *Journal of Fungi (Basel, Switzerland)*, *7*(8). https://doi.org/10.3390/JOF7080599

Zhang, J., Jimenez, L. L., Snelders, E., Debets, A. J. M., Rietveld, A. G., Zwaan, B. J., Verweij, P. E., & Schoustra, S. E. (2020). Dynamics of Aspergillus fumigatus in Azole Fungicide-Containing Plant Waste in the Netherlands (2016-2017). *Applied and Environmental Microbiology*, *87*(2), 1–12. https://doi.org/10.1128/AEM.02295-20/SUPPL_FILE/AEM.02295-20-S0001.PDF

Zhang, J., Li, L., Lv, Q., Yan, L., Wang, Y., & Jiang, Y. (2019). The fungal CYP51s: Their functions, structures, related drug resistance, and inhibitors. *Frontiers in Microbiology*, *10*, 436065. https://doi.org/10.3389/FMICB.2019.00691

Zhang, J., & Panthee, D. R. (2022). Next-generation sequencing-based bulked segregant analysis without sequencing the parental genomes. *G3 Genes|Genomes|Genetics*, *12*(2). https://doi.org/10.1093/G3JOURNAL/JKAB400

Zhang, J., Verweij, P. E., Rijs, A. J. M. M., Debets, A. J. M., & Snelders, E. (2022). Flower Bulb Waste Material is a Natural Niche for the Sexual Cycle in Aspergillus fumigatus. *Frontiers in Cellular and Infection Microbiology*, *11*, 785157. https://doi.org/10.3389/FCIMB.2021.785157/BIBTEX

Zhang, Y., Zhang, X., & Qiu, W. (2023). An efficient mutagenesis system to improve the propamocarb tolerance in Lecanicillium lecanii (Zimmermann) Zare & Gams. *Frontiers in Microbiology*, *14*. https://doi.org/10.3389/FMICB.2023.1243017

Zhao, L., Pridgeon, J. W., Becnel, J. J., Clark, G. G., & Linthicum, K. J. (2009). Mitochondrial Gene Cytochrome b Developmental and Environmental Expression in Aedes aegypti (Diptera: Culicidae). *Journal of Medical Entomology*, *46*(6), 1361–1369. https://doi.org/10.1603/033.046.0615

9 Annexes

Annex 1: Maximal Concentrations and Mechanistic Classifications of Antifungal Agents in Gradient Agar Assays*. An overview of antifungal concentrations and strategic grouping based on mode of action with corresponding literature references.*

Antifungal	Maximal Concentration (mg/L)	Group of fungicide	Reference
Itraconazole	16	DMI-fungicides (Demethylation Inhibitors) (SBI: Class I)	Guinea et al., 2019
Voriconazole	32	DMI-fungicides (Demethylation Inhibitors) (SBI: Class I)	Guinea et al., 2019
Posaconazole	2	DMI-fungicides (Demethylation Inhibitors) (SBI: Class I)	Snelders et al., n.d.
Tebuconazole	16	DMI-fungicides (Demethylation Inhibitors) (SBI: Class I)	Guinea et al., 2019
Azoxystrobin	32	QoI fungicides (Quinone outside Inhibitors)	Snelders et al., n.d.
Benomyl	2	MBC fungicides (Methyl Benzimidazole Carbamates)	Snelders et al., n.d.
Propamocarb	32	Carbamates	Zhang et al., 2023
Mancozeb	4	Chemicals with Multi-Site Activity M01	Piprotar et al., 2022
Copper(ii) sulphate 5-hydrate	4	Chemicals with Multi-Site Activity M03	Song et al., 2019
Copper(ii) sulphate anhydrous	4	Chemicals with Multi-Site Activity M03	Song et al., 2019
Acriflavine	5	Chemicals with Multi-Site Activity	Auxier et al., 2023
	20		
Carvacrol	10	Biologicals with Multiple Modes of Action BM1	Kocić-Tanackov et al., 2012
	150		

Annex 2: Inhibitory Profiles of Selected Antifungals on Aspergillus fumigatus Offspring Growth and Sporulation. *This table shows antifungal agents tested at varying concentrations against four phenotypes of A. fumigatus offspring: big with sporulation (BS), small with sporulation (SS), big non-sporulate (BN), and small non-sporulate (SN). It details the area of growth in cm² and the percentage of isolates with sporulation for each treatment group.*

		BS		SS		BS		SN		88C19		46A23	
Antifungal	Concetration (mg/L)	Area of growth (cm^2)	Percent with Sporulation	Growth	Percent with Sporulation	Growth	Percent with Sporulation	Growth	Percent with Sporulation	Growth	Percent with Sporulation	Growth	Percent with Sporulation
Control	-	1,3258	100	1,544	100	1,3431	100	1,1029	100	1,199	100	0,9775	100
Itraconazole	32	0,0995	0	0,1634	0	0,1084	0	0,1023	0	0	0	0,231	0
	16	0,1862	0	0,2626	0	0,144	0	0,1495	0	0	0	0,2909	0
Benomyl	20	0,2909	0	0,2913	0	0,036	0	0,0363	0	0	0	0,207	0
	16	0,3159	0	0,4244	0	0,1044	0	0,1352	0	0,122	0	0,262	0
Mancozeb	16	0,6031	80	0,5331	80	0,1965	30	0,1377	10	0	0	0	0
	8	1,0585	100	1,0072	90	0,5045	60	0,4322	50	0,4035	0	0,62	0
Tebuconazole	16	0,2744	30	0,346	70	0,5016	70	0,1611	60	0	0	0,8395	0
	8	0,555	50	1,2667	90	0,8793	100	0,8891	90	0	0	1,925	100
Acriflavine	100	0,2857	100	0,2668	100	0,0354	30	0,0462	40	0	0	0	0
	15	0,7936	100	0,6545	100	0,3144	70	0,2305	70	0	0	0,481	100

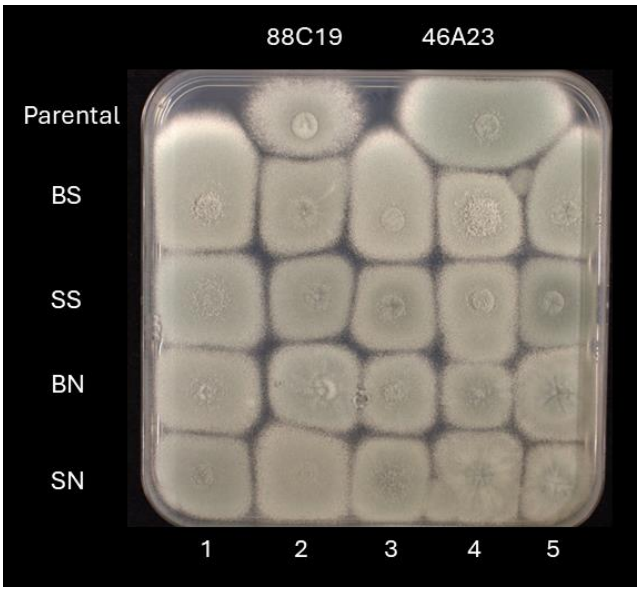

Annex 3: Azoxystrobin Susceptibility Test on A. fumigatus Offspring and Parental Strains*. The susceptibility test was performed on high concentrations of azoxystrobin. The first row has both parentals 88C19 (azole-susceptible) and 46A23 (azole-resistance). The next rows represent a different phenotype: big with sporulation (BS), small with sporulation (SS), big non-sporulate (BN), and small non-sporulate (SN). As all the samples were able to grow and no significant difference was observed, the results for these samples were not statically analyzed.*

Annex 4: Quantitative and Qualitative Analysis of DNA Samples from A. fumigatus Offspring for Nanopore Sequencing*. Here the concentration of double-stranded DNA (dsDNA) for sequencing is quantified using a Qubit fluorometer (in ng/µL). Additionally, the table includes optical density (OD) ratios at A260/230 and A260/280, measured by Nanodrop to assess purity. The integrity of the DNA is evaluated by the presence and pattern of bands following agarose gel electrophoresis.*

Sample	dsDNA concentration (ng/µl)	OD at A260/230	OD at A260/280	Integrity in agarose gel
BS	47,4	1,71	1,999	Single band above 10 kb
SS	37,8	2,029	1,97	Sample is highly degraded
BN	19,4	1,721	1,721	No band
SN	32	2,127	1,979	Single band above 10 kb

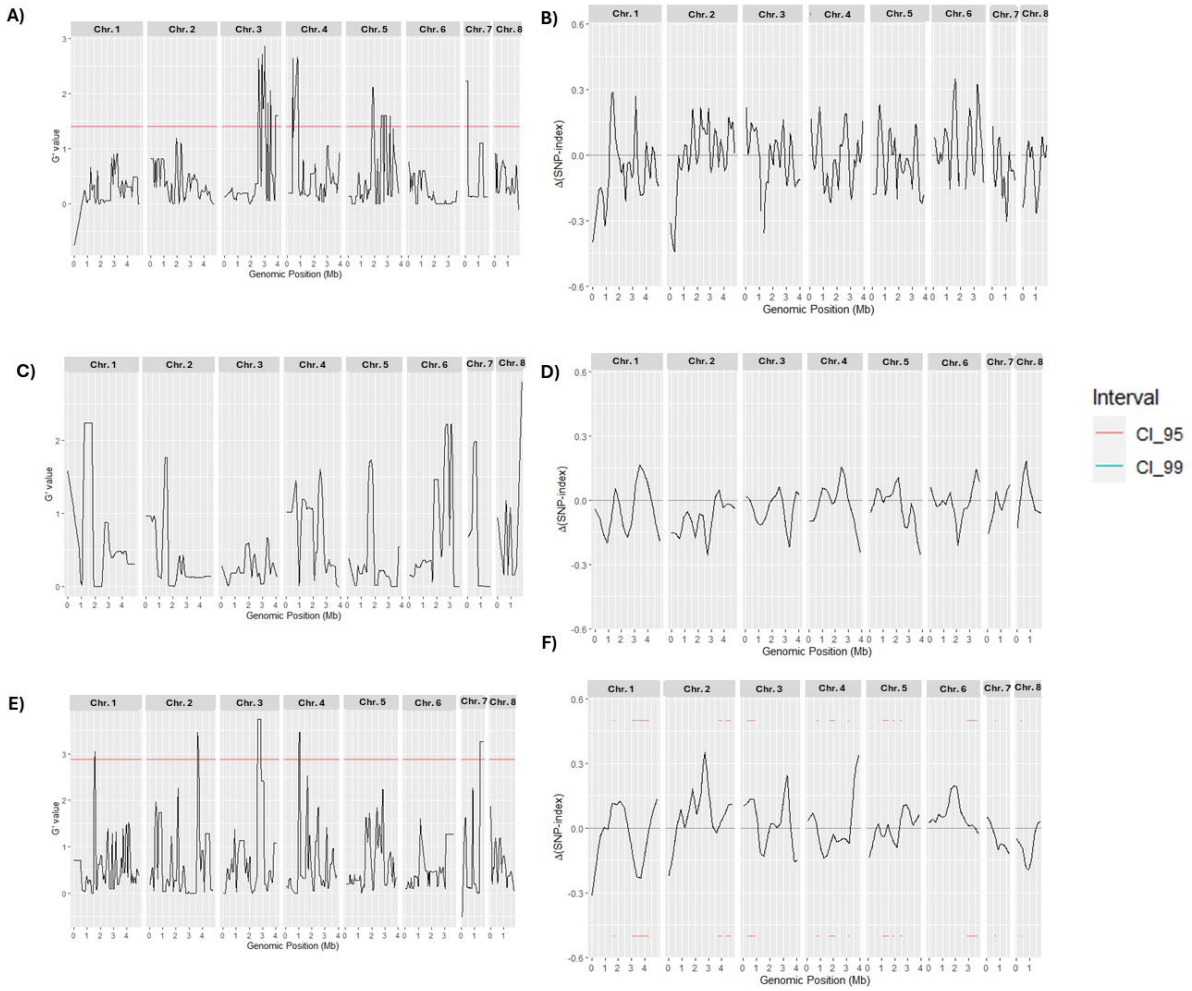

Annex 5: QTL-seq Analysis of A. fumigatus Offspring*. The figure presents the results of a QTL-seq analysis, showcasing significant G' values and ΔSNP index across eight chromosomes of A. fumigatus. Graphs A and B illustrate G's values and ΔSNP index for high bulk BS against low bulk*

SN; C and D display these metrics for high bulk BS against low bulk SD; E and F represent high bulk SS against low bulk SN. Confidence intervals are denoted by red lines at 95% (CL_95) and 99% (CL_99) thresholds. These graphs were generated using sequencing data obtained from Nanopore technology.

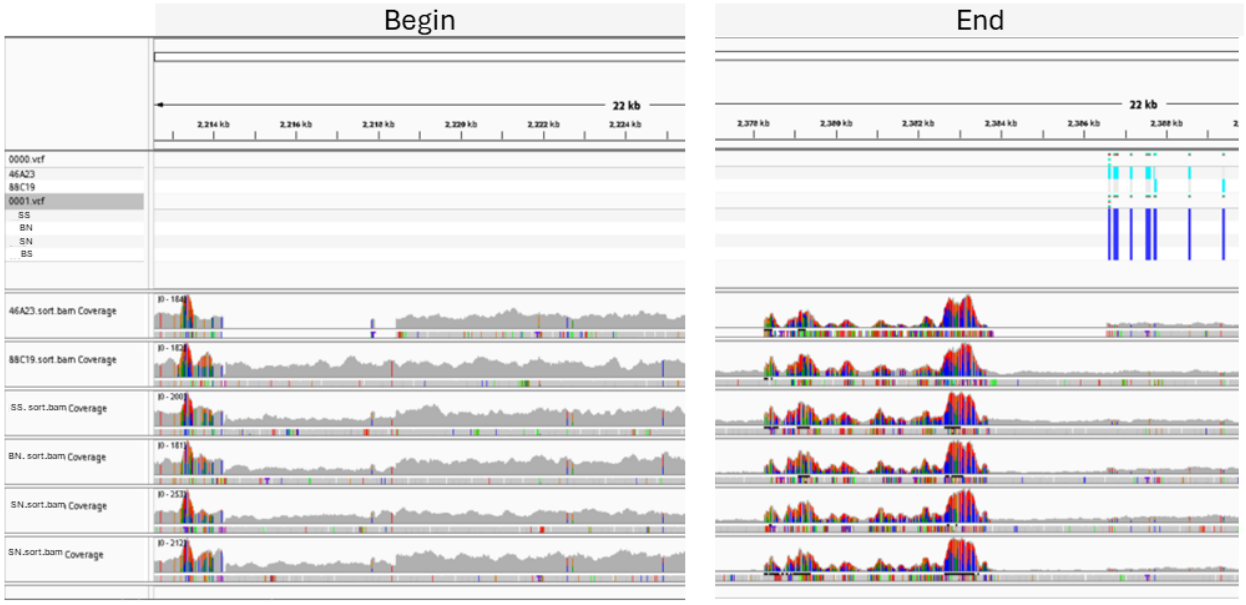

Annex 6: Integrative Genomics Viewer (IGV) Snapshot of SNP Distribution and Read Depth in QTL of chromosome 6*. This IGV snapshot provides a comparative visualization of SNP distribution and read depth across a specific genomic region with low coverage. The image illustrates the sequences of parental strains 46A23 and 88C19, along with four phenotypic offspring variants (BS, SS, BN, SN). The left side ('Begin') of the image represents the start of the genomic region, while the right side ('End') details the culmination of the region, highlighting read numbers in this region.*